Journal of Thermal Analysis and Calorimetry, Vol. 55 (1999) 271-282

Al–Zn–Sn PHASE DIAGRAM
Calorimetric study of the isobaric invariants

E. Aragon[1*], *D. Vincent*[2], *A. M. Zahra*[3] *and A. Sebaoun*[1]

[1]Laboratoire de Physico-Chimie du Matériau et du Milieu Marin, Matériaux à Finalité Spécifique (E. A. 1356), Université de Toulon et du Var, B. P. 132, 83957 La Garde cedex France
[2]S. A. Metalor, av. du Vignoble, CH-2009 Neuchâtel, Switzerland
[3]Centre de Thermodynamique et de Microcalorimétrie du CNRS, 26 rue du 141 R.I.A. 13331 Marseille cedex 3, France

(Received December 1, 1997)

Abstract

A systematic study of Al–Zn–Sn ternary alloys by using a Tian-Calvet calorimeter with slow heating and cooling rate was carried out and supplemented by scanning electron microscopic observations.

The results have shown that crystallization coupled with dissolution of tin into the α'_{SS} ternary solid solution on heating is an endothermic process, while melting coupled with tin expulsion on cooling is an exothermic one. It seems that the thermal effects of phase transition are outweighed by much stronger ones due to a large composition change of the α'_{SS} ternary phase.

Keywords: Al–Zn–Sn ternary system, calorimetric measurements, crystallization, invariant reaction, mixing enthalpies, phase diagram, Tammann method

Introduction

In previously published papers [1–7], we have proposed an Al–Zn–Sn phase diagram (Fig. 1a) showing all isobaric liquid–solid and solid–solid equilibria. In those papers, the stability fields of the phases in equilibrium as well as the ternary isobaric invariants were determined or more accurately investigated (Figs 1b–d). Studies were done by the isopleth cutting method using coupled direct and differential thermal analysis, metallographic observations, electron probe microanalysis for the examination of the phases formed by isothermal diffusion [1–6], more recently X-ray diffraction at various temperatures and thermodilatometric measurements in the ternary system [6, 7].

* Author for corrspondence:phone: 33-4-94-14-23-05; fax: 33-4-94-14-23-42;
e-mail: Ipcm3@univ-tln.fr

1418–2874/99/ $ 5.00
© 1999 Akadémiai Kiadó, Budapest
Akadémiai Kiadó, Budapest
Kluwer Academic Publishers, Dordrecht

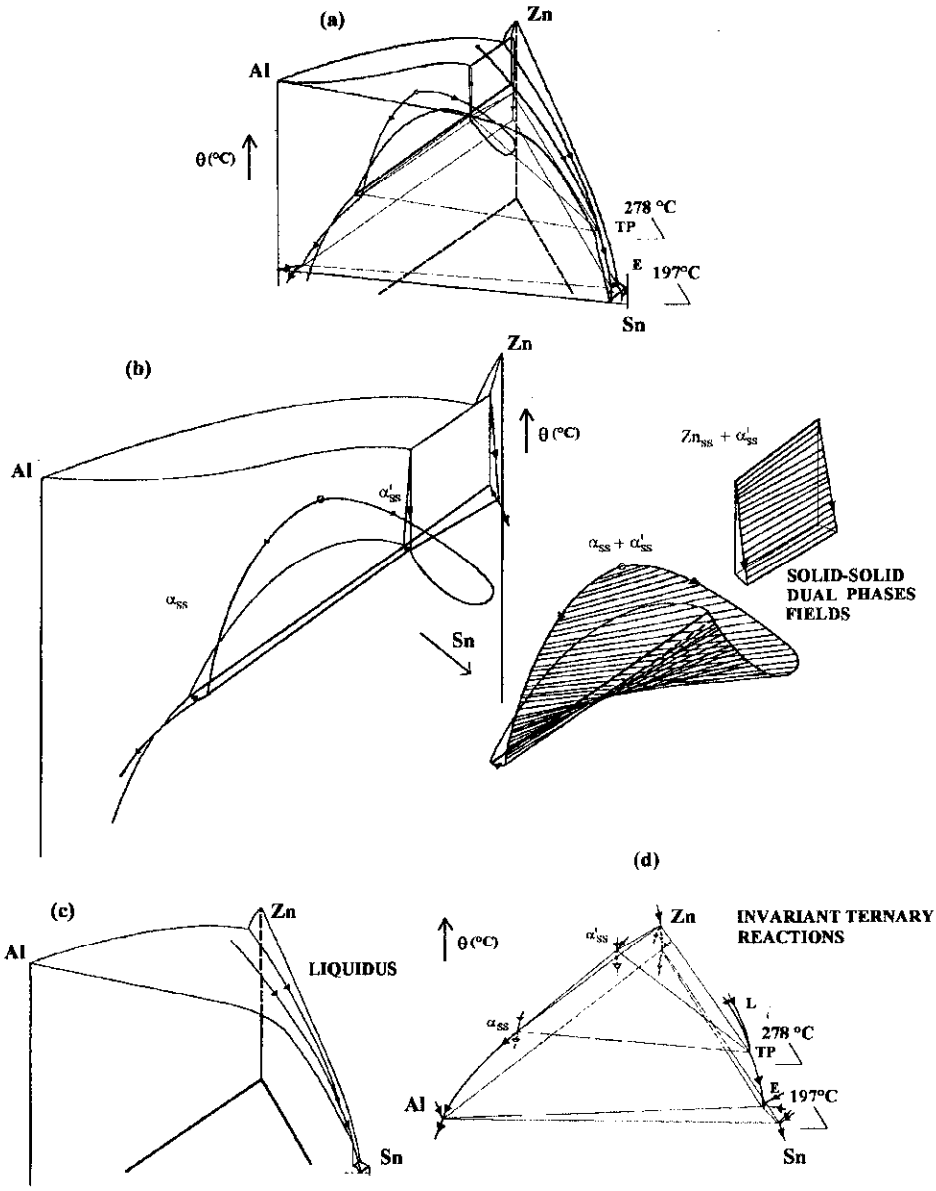

Fig. 1 Al–Zn–Sn diagram: (a) complete diagram; (b) solidus area: solid solution showing retrograde miscibility of tin, critical point (446°C) on α_{ss}–α'_{ss} solid solution miscibility gap (perspective view); (c) liquidus area with monovariant curves, one of which exhibits a vanishing point (446°C) conjugated with the solid–solid critical point (perspective view); (d) ternary isobaric invariant reactions: eutectic (E) at 197°C, transitory peritectic (TP) at 278°C, monovariant lines associated with $\alpha_{ss}+\alpha'_{ss}+L'$ and $Zn_{ss}+\alpha'_{ss}+L$ (perspective view)

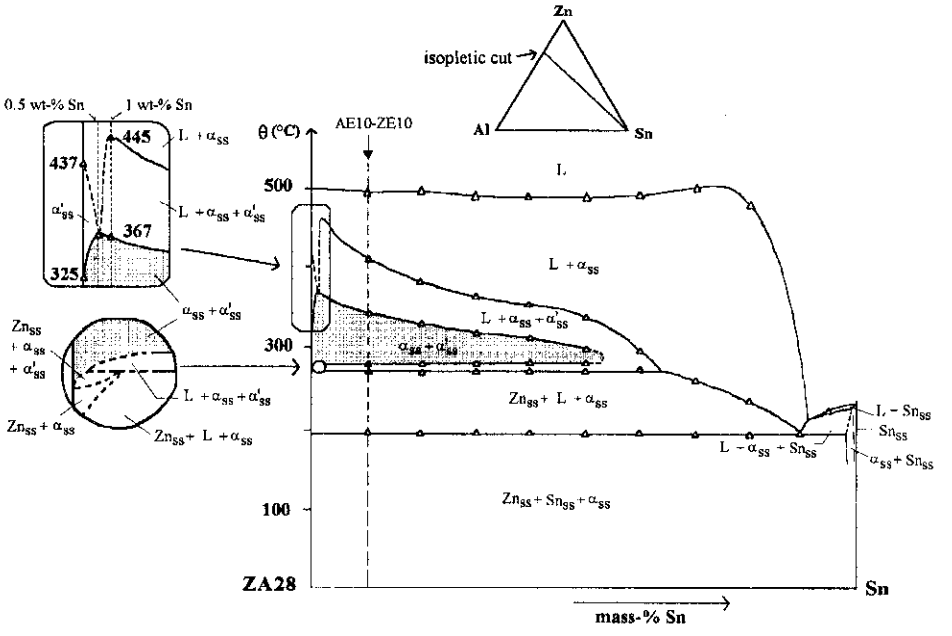

Fig. 2 Al–Zn–Sn phase diagram: ZA28–Sn isopletic cut. Temperatures obtained by DTA [4]

On heating, a ternary isobaric eutectic reaction (E) occurs at 197°C:

$$Sn_{SS} + Zn_{SS} + \alpha_{SS} \rightleftarrows L \qquad \Delta H^{\circ}_{E} > 0$$

where ΔH°_{E} is the enthalpy.

Figures 1b, 2 and 3 show the existence of a solid solution α'_{SS} extending in the direction of high concentration of tin and exhibiting a significant retrograde miscibility for tin. On each side of the solid solution, for zinc concentrations varying from 30 to 99%* and temperatures higher than about 286°C, the two solid–solid dual phase fields correspond respectively to:

$$\alpha'_{SS} + \alpha_{SS} \quad \text{and} \quad \alpha'_{SS} + Zn_{SS}$$

with liquids, these solid phases give the two solid–solid–liquid phase fields:

$$L + \alpha'_{SS} + Zn_{SS} \quad \text{and} \quad L' + \alpha'_{SS} + \alpha_{SS}$$

The liquids L and L' correspond in Fig. 1d to the monovariant lines which converge at 278°C. At this temperature an invariant isobaric reaction occurs which is a transitory peritectic (TP) [8–11]:

* The compositions will always be given in mass percent

$$Zn_{SS} + \alpha_{SS} \rightleftarrows L + \alpha'_{SS} \qquad \Delta H^{o}_{TP} > 0$$

Between 284 and 286°C, depending on the tin concentration, and up to 30% of tin on the isopletic cut ZA28-Sn (m_{Al}/m_{Zn}=0.39) (Fig. 2), the following reaction occurs which corresponds to crystallization (C) on heating and fusion on cooling

$$L \rightleftarrows \alpha'_{SS} + \alpha_{SS} \qquad \Delta H^{o}_{C}$$

As the two reactions, (TP) and (C) are very close to each other, the thermal analysis curves cannot return to the base line in the temperature range 278–286°C. Figure 4 shows an example of a thermal curve and the difficulty of its interpretation due to tin dissolution on heating.

These curves do not allow to decide whether the crystallization reaction occurring on heating is actually associated with an exothermic effect superimposed on an endothermic one, or whether two endothermic effects overlap. Hence, a more systematic calorimetric study was undertaken and supplemented by Scanning Electron Microscopic (SEM) investigations.

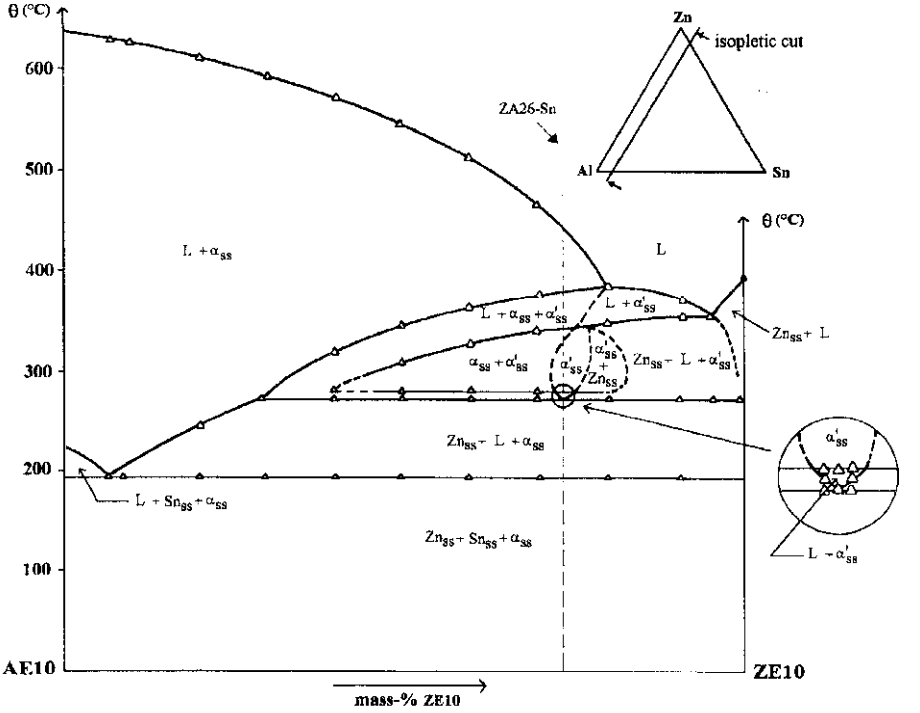

Fig. 3 Al–Zn–Sn phase diagram: AE10–ZE10 isopletic cut. Temperatures obtained by DTA [4]

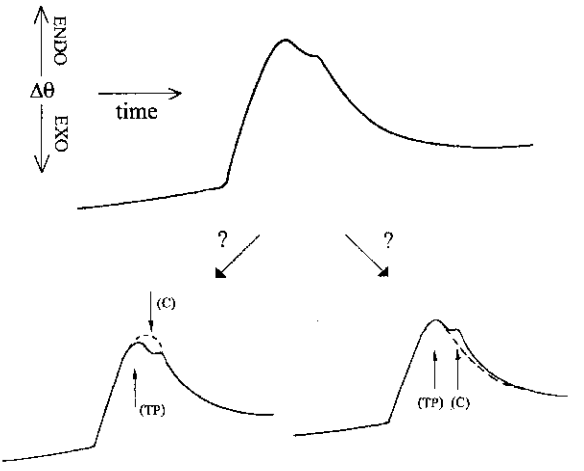

Fig. 4 Al–Zn–Sn phase diagram: DTA curves [4] on heating for a sample containing 42% of aluminium on the AE10–ZE10 isopletic cut

Experimental

The Tammann method has been proposed for binary systems [9, 12–14] for which only one composition is an independent variable because of the normalization of the compositions (X_A=1–X_B). In this case, a quasi linear change of the enthalpy associated with an invariant transformation occurs as a function of the composition (for a representation in mass percent). A similar method has been described for some particular and theoretical cases of ternary systems [15], but little experimental work has been done on this topic [16, 17].

In ternary systems, two compositions are independent (X_A+X_B=1–X_c); the enthalpy associated with an invariant transformation may linearly vary as a function of the proportion of the invariant phase(s) formed (or decomposed). As a consequence, the heat evolution has to be followed as a function of two composition directions: on the AE10–ZE10 (m_{Sn}=10, 0≤m_{Zn}≤90) and ZA26–Sn (m_A/m_{Zn}=0.35, 0≤m_{Sn}≤100) isopletic cuts. On these cuts, nine alloys have been studied (Fig. 5):

Calorimetric measurements were carried out on the two isobaric invariants: first, on the eutectic transformation (E) in order to validate the experimental approach, and secondly, on the peritectic transformation (TP) associated with the α'_{SS} crystallization (C) on heating. A differential Tian-Calvet calorimeter was used. Its sensitivity was 0.01 V W^{-1} at 275°C.

The samples were prepared by weighing, mixing and casting pure Al, Zn and Sn (99.999%) in cast iron crucibles under a nitrogen atmosphere in order to obtain a cylindric ingot (φ:15.6±0.1 mm; *h*: 70 mm) with a mass of about 50 to 65 g.

Table 1 Compositions studied on the ZA26–Sn and AE10–ZE10 isopletic cuts

Sample	Isopletic cut	Compositions/mass%		
		Al	Zn	Sn
1	ZA26–Sn	24.7	70.3	5
3		20.8	59.2	20
4		10.4	29.6	60
2	ZA26–Sn/AE10–ZE10	23.4	66.6	10
5	AE10–ZE10	21.6	68.4	10
6		36	54	10
7		49.5	40.5	10
8		58.5	31.5	10
9		63	27	10

The heating and cooling rate was chosen about 10 K h^{-1}. Measurements were repeated many times both on heating and cooling in order to verify the reversibility and the reproducibility of the phenomena.

The integration of the thermal curves is difficult because of the variation of heat capacity during the transformations. As a consequence, the accuracy of the enthalpy measurements is only about 90%.

In addition, electron microprobe analysis was used in the present investigations.

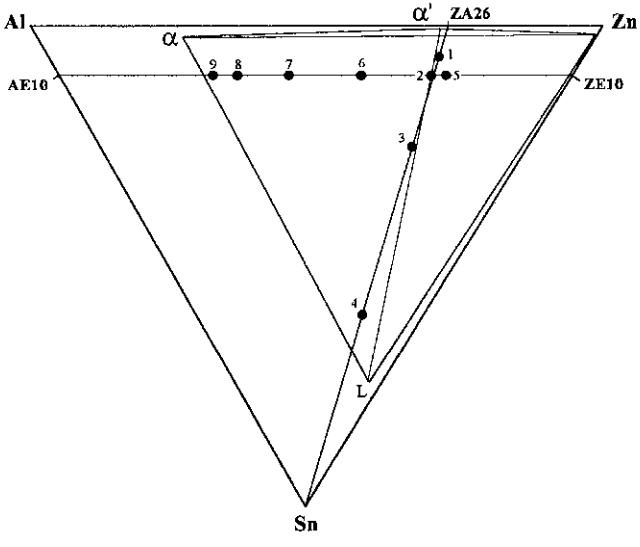

Fig. 5 Al–Zn–Sn phase diagram: transitory peritectic reaction (TP) at 278°C [4] and compositions studied on the ZA26–Sn and AE10–ZE10 isopletic cuts

Results

Temperature determination

The temperatures determined in Tian-Calvet calorimetry are only slightly different from those determined by DTA [4] as shown in Table 2. These values are in a good agreement despite the differences in heating rates and experimental methods.

Table 2 Temperatures of the invariant reactions and of the crystallization of the α′ phase obtained on heating by Tian-Calvet calorimetry and DTA [4]

	Tian-Calvet Calorimetry	DTA [4]
Eutectic (E)	196°C	197°C
Transitory peritectic (TP)	275–276°C	278°C
Crystallization of the α′ phase (C)	283°C	286°C

Ternary eutectic invariant reaction

In order to check the efficiency of the Tammann method, the calorimetric measurements obtained on the ternary eutectic reaction were evaluated. The re-

Table 3 Measured enthalpies (J g^{-1}, ±10%) associated with the invariant reactions and with the crystallization of the α′ phase during heating

					ZA26		
					1		
				Eutectic	3.9		
				Peritectic	23.7		
				Crystallization	1.5		
AE10	9	8	7	6	2	5	ZE10
Eutectic	8	8.7	7.8	8.8	7.1	8.4	
Peritectic	1.3	3.7	6.7	9.5	35.1	17.3	
Crystallization	/	0.3	2.8	3.3		0.1	
					3		
				Eutectic	18.9		
				Peritectic	10.9		
				Crystallization	1.4		
					4		
				Eutectic	51.8		
				Peritectic	4.7		
				Crystallization	/		
					Sn		

sults are given in Table 3 and the enthalpy variations as a function of composition on the ZA26–Sn and AE10–ZE10 isopletic cuts are presented in Fig. 6.

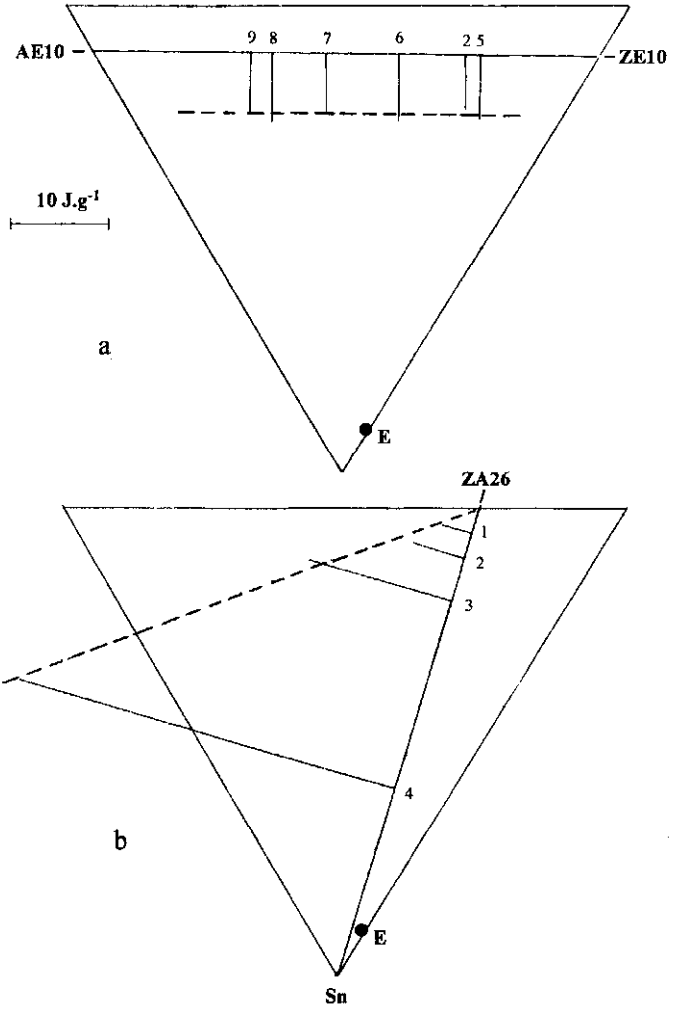

Fig. 6 Al–Zn–Sn phase diagram: evolutions of the enthalpies for the ternary eutectic reaction (E) at 197°C on the AE10–ZE10 (a) and ZA26–Sn (b) isopletic cuts

On the AE10–ZE10 isopletic cut, the proportion of the formed eutectic liquid is constant for all the alloys and the measured heats are the same (about 8.1 ± 0.8 J g^{-1}). On the ZA26–Sn isopletic cut, the enthalpy is linearly increasing with decreasing distance of the considered composition from the eutectic point. These findings justify our experimental approach.

Ternary peritectic invariant reaction and α'_{SS} crystallization

On the same isopletic cuts, with the same mixtures, we studied the heat effects due to reactions (TP) and (C). In Fig. 7, the curves obtained for different compositions on the ZA26–Sn and AE10–ZE10 isopletic cuts are shown. Alloys 4 and 9 do not exhibit the crystallization (C) of the α'_{SS} phase on heating. We also observed that the two phenomena, (TP) and (C), cannot be separated in the case of alloy 2. For all mixtures, we found that $|\Delta H^{\circ}_{TP}| >> |\Delta H^{\circ}_{C}|$ and that ΔH°_{TP} is evidently endothermic.

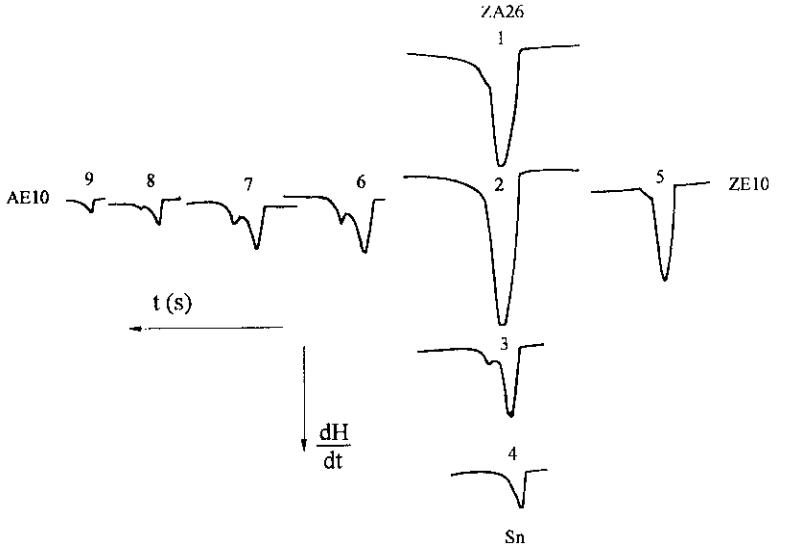

Fig. 7 Al–Zn–Sn phase diagram: calorimetric curves for the transitory peritectic invariant reaction (TP) at 278°C on the ZA26–Sn and AE10–ZE10 isopletic cuts

The next question to answer was of whether the α'_{SS} crystallization on heating manifests itself as an exothermic or an endothermic process. ΔH°_{C} values were first calculated by supposing that the transformation is an endothermic process on heating, i.e. $\Delta H^{\circ}_{C}>0$. The enthalpy values for ΔH°_{C} and ΔH°_{TP} are given in Table 3. The higher the aluminium content (from 2 to 8 on the AE10–ZE10 isopletic cut and from 2 to 3 on the ZA26–Sn isopletic cut: Fig. 7), the easier it is to separate the two thermal effects.

The heat evolutions on the ZA26–Sn and AE10–ZE10 isopletic cuts are shown in Fig. 8. The measured global heat for mixture 2 is greater than the extrapolated heat associated with the single peritectic reaction on the two cuts. As a consequence, the signs of the two thermal effects are identical and positive. This conclusion, which corresponds to our initial hypothesis, shows that crystallization (C) is apparently an endothermic process on heating.

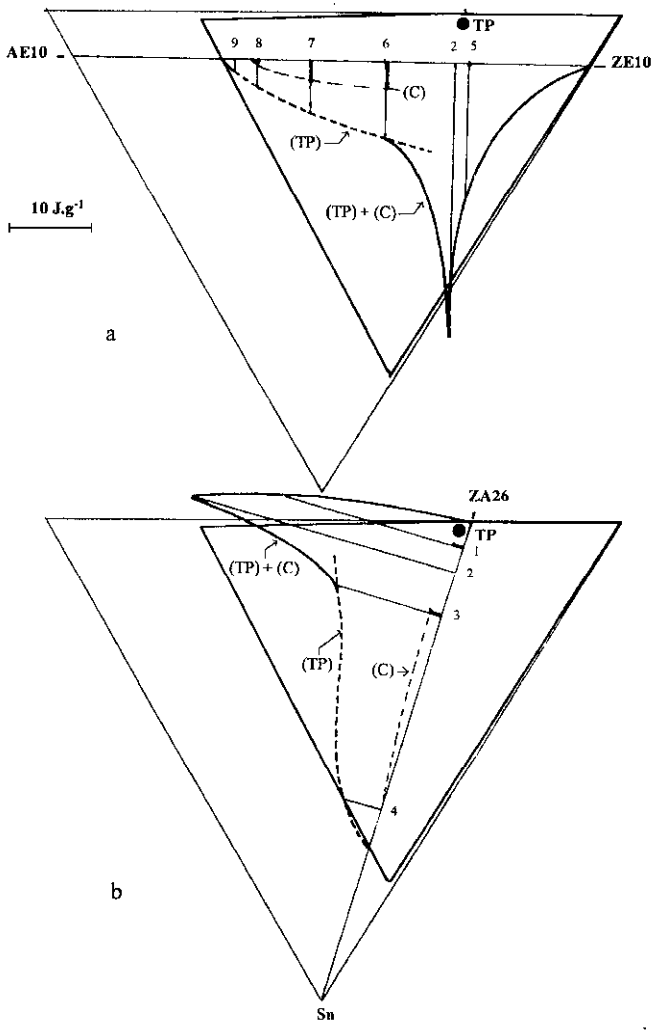

Fig. 8 Al–Zn–Sn phase diagram: heat evolution for the ternary peritectic reaction (TP) at 278°C and for the α'_{SS} crystallization (C) on heating on the AE10–ZE10 (a) and ZA26–Sn (b) isopletic cuts

Crystallization, however, is always an exothermic process. It is thus suggested that the α'_{SS} crystallization corresponds to a complex process which includes two different phenomena: a crystallization associated with an exothermic effect ($\Delta H^{\circ}_{CRYST}<0$) and a simultaneous dissolution of tin associated with an endothermic phenomenon ($\Delta H^{\circ}_{SOL}>0$). It seems that the thermal effect of phase transition is outweighed by a much larger effect due to a significant change in the composition of the α' ternary phase.

SEM investigation

Supplementary investigations were performed by SEM in order to elucidate the mechanism of processes occurring during melting and cooling. Figure 9 shows the scanning electron micrograph and a tin-specific picture obtained by electron probe microanalysis, taken at room temperature after quenching from an annealing temperature of 300°C of a sample containing 42% of tin on the AE10–ZE10 isopletic cut.

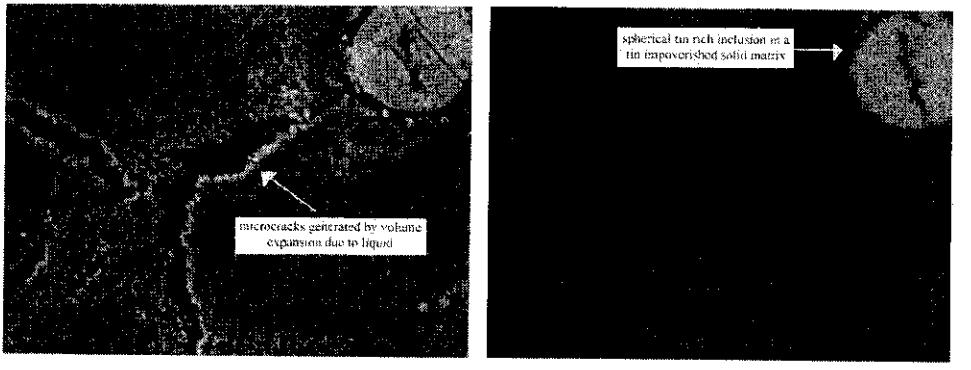

Fig. 9 Al–Zn–Sn phase diagram: Scanning electron micrograph (9a) and tin-specific picture obtained by electron probe microanalysis (9b) for a sample containing 42% of aluminium on the AE10–ZE10 isopletic cut, at room temperature after quenching from an annealing temperature of 300°C; (Acc. V: 30 kV; Magn.: ×800; Det: B.S.E.)

The retrograde solubility of the α' solid solution towards tin induces a tin expulsion when the samples are cooled. This tin rejection occurs in the temperature range where tin is liquid: consequently we observe a spherical localized inclusion of tin. Liquid expulsion corresponds to a volume expansion in a solid matrix and generates microfractures in the α/α' interface. When this liquid crystallizes, the contraction will generate holes in α'. As a consequence, these phase transitions do not take place under isobaric condtitions.

A hole and microfracture formation mechanism in the Al–Zn–Sn alloys has already been proposed [4]. Holes and microfractures deteriorate the mechanical properties and increase the corrosion sensitivity of these alloys.

Conclusions

This calorimetric study in the Al–Zn–Sn ternary phase diagram has shown that crystallization coupled with dissolution of tin into the α'_{ss} ternary solid solution on heating is an endothermic process, while melting coupled with tin expulsion on cooling is an exothermic one. It seems that the thermal effects due to a phase transition are outweighed by much larger effects due to a significant

change in the composition of the α'_{ss} ternary phase. These phenomena are then very complex and the equilibria difficult to model.

The consequences of these phenomena were checked by SEM. The observations show that the transformations do not take place under isobaric conditions. A supplementary study under different pressures may improve the understanding of the equilibria in the Al–Zn–Sn ternary system.

References

1 D. Vincent, D. E. S., No. 84, Université Claude Bernard, Lyon I, France 1980.
2 D. Vincent and A. Sebaoun, J. Thermal Anal., 20 (1981) 419.
3 D. Vincent and A. Sebaoun, Mém. Etud. Sci. Rev. Métall., 78 (1981) 165.
4 D. Vincent, Contribution à l'Etude du Système ternaire Al–Zn–Sn, Thesis, No. 81, Université Claude Bernard, Lyon I, France 1982.
5 A. Sebaoun, D. Vincent and D. Treheux, Materials Science and Technology, 3 (1987) 241.
6 E. Aragon and A. Sebaoun, 'Al–Zn–Sn Phase Diagram: X-ray diffraction study at various temperatures', J. Thermal Anal., to be published.
7 E. Aragon, Etude d'Alliages d'Aluminium pour la Protection Cathodique de Structures en Eau de Mer, Université de Toulon et du Var, France 1995.
8 R. Cayron, Etude et Théorie des Diagrammes d'Equilibre dans les Systèmes Quaternaires, Vol. 1, Louvain, Belgium, Institut de Métallurgie, 1960, p. 15.
9 A. P. Rollet and R. Bouaziz, L'Analyse Thermique, Gauthier Villars ed., Paris 1972.
10 J. Postma, Rec. Trav. Chim., 39 (1920) 515.
11 F. N. Rhines, Phase Diagrams in Metallurgy: their Delevopment and Application, New York, McGraw-Hill ed., 1956, p. 176.
12 G. Tammann, Z. Phys. Chem., 37 (1903) 303.
13 G. Tammann, Z. Phys. Chem., 45 (1905) 24.
14 G. Tammann, Z. Phys. Chem., 47 (1905) 289.
15 R. Sahmen and A. Vegesack, Z. Phys. Chem., 59 (1907) 257.
16 V. R. Loebe, Metallurgie, 8 (1911) 7.
17 G. Tammann and O. Dahl, Z. anorg. all. Chem., 144 (1925) 1.